

# 11. Hasil uji similaritas Muscle-Guided Mapping

*by Erica Kholinne*

---

**Submission date:** 10-Feb-2025 08:26PM (UTC+0700)

**Submission ID:** 2477749668

**File name:** eterotopic\_Ossification\_of\_the\_Elbow\_\_A\_Novel\_CT-Based\_Study.pdf (746.62K)

**Word count:** 5959

**Character count:** 41120

# Journal Pre-proof

Muscle-Guided Mapping of the Post-Traumatic Heterotopic Ossification of the Elbow:  
A Novel CT-Based Study

Jia Guo, MD, Erica Kholinne, MD PhD, Jiyeon Park, MD, Hui Ben, MD PhD, In-Ho Jeon, MD, PhD

PII: S1058-2746(25)00073-4

DOI: <https://doi.org/10.1016/j.jse.2024.12.013>

Reference: YMSE 7218



To appear in: *Journal of Shoulder and Elbow Surgery*

Received Date: 11 July 2024

Revised Date: 19 November 2024

Accepted Date: 8 December 2024

Please cite this article as: Guo J, Kholinne E, Park J, Ben H, Jeon I-H, Muscle-Guided Mapping of the Post-Traumatic Heterotopic Ossification of the Elbow: A Novel CT-Based Study, *Journal of Shoulder and Elbow Surgery* (2025), doi: <https://doi.org/10.1016/j.jse.2024.12.013>.

This is a PDF file of an article that has undergone enhancements after acceptance, such as the addition of a cover page and metadata, and formatting for readability, but it is not yet the definitive version of record. This version will undergo additional copyediting, typesetting and review before it is published in its final form, but we are providing this version to give early visibility of the article. Please note that, during the production process, errors may be discovered which could affect the content, and all legal disclaimers that apply to the journal pertain.

© 2025 Published by Elsevier Inc. on behalf of Journal of Shoulder and Elbow Surgery Board of Trustees.

**Muscle-Guided Mapping of the Post-Traumatic Heterotopic Ossification of the Elbow: A Novel CT-Based Study**

*Running title: Muscle-Guided Mapping for Post-Traumatic Heterotopic Ossification*

Jia Guo MD<sup>1</sup>, Erica Kholinne, MD PhD<sup>2</sup>, Jiyeon Park MD<sup>1</sup>, Hui Ben MD PhD<sup>1</sup>, In-Ho Jeon, MD, PhD<sup>1</sup>

1. Department of Orthopedic surgery, Asan Medical Center, University of Ulsan College of Medicine, Seoul, Republic of Korea
2. Faculty of Medicine, Universitas Trisakti, Department of Orthopedic Surgery, St. Carolus Hospital, Jakarta, Indonesia

**Corresponding author:** In-Ho Jeon, MD, PhD, Department of Orthopaedic Surgery, Asan Medical Center, University of Ulsan College of Medicine, 88 Olympic-ro 43-gil, Songpa-gu, Seoul 05535, Korea

Tel: +82-2-3010-3530; Fax: +82-2-488-7877; E-mail: [jeonchoi@gmail.com](mailto:jeonchoi@gmail.com)

Asan Medical Center institutional review board approved this study (approval no. 2024-1302).

**Disclaimers:**

Funding: No funding was disclosed by the authors.

Conflicts of interest: In-Ho Jeon serves as an Associate Editor for the *Journal of Shoulder and Elbow Surgery*. The other authors, their immediate families, and any research foundation with which they are affiliated have not received any financial payments or other benefits from any commercial entity related to the subject of this article.

1 **Muscle-Guided Mapping of the Post-Traumatic Heterotopic Ossification of the**  
2 **Elbow: A Novel CT-Based Study**

3 *Running title: Muscle-Guided Mapping of Post-Traumatic Heterotopic Ossification*

4

5 **Abstract**

6 **Background:** Heterotopic ossification (HO) involves abnormal bone formation in soft  
7 tissues near joints, commonly occurring after elbow trauma or surgery, leading to pain  
8 and functional limitations. Previous studies have primarily characterized HO  
9 distribution based on bony landmarks, lacking a detailed investigation into the  
10 characteristics of its distribution in periarticular soft tissue in post-traumatic elbows.  
11 This study aimed to (1) develop a muscle-guided classification system using computed  
12 tomography (CT) to map HO relative to elbow muscle-tendon units and (2) investigate  
13 correlations between HO location and severity.

14 **Methods:** In a retrospective study, 56 patients with HO and elbow stiffness following  
15 trauma were analyzed. CT imaging was used to classify HO into seven categories:  
16 Posterior - olecranon tip - triceps brachii (P-O-T); Posteromedial - medial gutter - flexor  
17 carpi ulnaris (PM-MG-FCU); Posterolateral - lateral gutter – anconeus (PL-LG-AN);  
18 Medial - medial epicondylar – flexor muscles (M-ME-FLEX); Lateral - lateral  
19 epicondylar – extensor muscles (L-LE-EXT); Anterior - humeroulnar joint – brachialis  
20 (A-HU-B); and Anterior - humeroradial – supinator (A-HR-SP). HO severity was  
21 graded (1-3) based on CT morphology, and correlations between HO location and  
22 severity were assessed.

23 **Results:** PM-MG-FCU was the most common HO location (67.9%). Significant  
24 correlations were found between HO severity and location, with higher rates of HO in  
25 grades 2 and 3, characterized by extensive mature bone formation and bone bridge  
26 development occurring in the PL-LG-AN, P-O-T, and PM-MG-FCU.

27 **Conclusion:** The muscle-guided classification system effectively delineated HO  
28 distribution near elbow muscle-tendon units. HO locations surrounding the anconeus,  
29 triceps brachii, and FCU (flexor carpi ulnaris) correlate with higher radiographic  
30 severity, providing valuable insights for treatment strategies.

31 **Keywords:** Elbow trauma; heterotopic ossification; elbow stiffness; radiographic  
32 severity; muscle-guided; classification; distribution prevalence

33 **Level of evidence:** Level IV; Case Series; Development of Classification System

34

35

36 Heterotopic ossification (HO) is a dynamic, complex pathologic process of ectopic  
37 bone formation in periarticular soft tissues.<sup>8</sup> It often occurs after trauma, burns, brain  
38 injuries, or surgical procedures, frequently affecting the hip, knee, and elbow joints.<sup>7</sup>

39 Although the exact pathogenesis of HO formation remains unclear, it is commonly  
40 considered that musculoskeletal injuries and postsurgical changes induce aberrant  
41 differentiation of mesenchymal stem cells.<sup>17</sup> This results in the pathological formation  
42 of cartilage and bone growth within soft tissues such as tendons, ligaments, and muscles,  
43 outside the native skeleton.<sup>8, 17</sup> The process may be influenced by the products of torn  
44 muscle, torn soft tissue, and bleeding following trauma.<sup>6</sup>

45 The formation of HO in the elbow joint can cause pain and functional impairment,  
46 significantly affecting the quality of life of patients. Direct trauma is the most common  
47 cause of HO in the elbow.<sup>14</sup> The prevalence of HO with functional limitation after elbow  
48 trauma is 20%.<sup>12</sup> Foruria et al proposed that HO in the post-traumatic elbow is  
49 preferentially located at the origin of soft-tissue structures near fracture sites, and it is  
50 particularly more frequent in areas where the soft tissue is damaged.<sup>12</sup> This suggests  
51 that the formation and growth of HO likely occur at specific locations within the soft  
52 tissue. Nevertheless, the authors did not indicate a specific location.

53 A recent animal study revealed that an injured Achilles tendon can be affected by HO,  
54 which presents specific spatiotemporal characteristics during the tendon healing  
55 process. A small HO initially deposits in the stump close to the bone, then near the  
56 muscle, and then extends in the direction of the tendon's main axes. These  
57 characteristics of HO formation in a healing Achilles tendon are also commonly  
58 observed in humans.<sup>29</sup>

59 However, few studies have investigated the characteristics of HO distribution in relation  
60 to the surrounding periarticular soft tissues in the post-traumatic elbow. To our  
61 knowledge, the distribution of HO in the post-traumatic elbow has previously been  
62 described only based on plain radiographic studies using two-dimensional bony  
63 landmarks.<sup>4, 15, 22, 33</sup> However, a classification that illustrates the relationship between  
64 HO characteristics and the soft tissue involved is lacking. Muscle-tendon units, which  
65 are directly involved in joint movement and stabilization with clear tendinous insertions  
66 on the bone, can serve as the main pathologic landmarks to classify elbow HO.<sup>3, 13, 20,</sup>

67 25, 26, 28

68 This study aimed to achieve two primary purposes: (1) to develop a novel muscle-  
69 guided classification system based on computed tomography (CT) images that precisely  
70 describes the positional relationship between HO and periarticular muscle-tendon units,  
71 and (2) to investigate the distribution characteristics of HO near muscle-tendon units in  
72 a post-traumatic stiff elbow and the correlation between HO location and radiographic  
73 severity. This knowledge may enhance the understanding of HO location in soft tissue  
74 and provide new treatment strategies such as optimizing the preoperative surgical plan,  
75 guiding surgical approaches for HO removal, and assisting the decision between  
76 arthroscopic and open procedures considering the available operational area.

77

78

## 79 **Methods**

### 80 **Participants**

81 The present retrospective investigation obtained ethical commission approval from the  
82 institutional review board of Asan Medical Centre (no. 2024-1302). An informed  
83 consent form was signed by the subjects.

84 The institutional case database was queried to identify all patients who underwent  
85 surgical treatment for symptomatic post-traumatic stiff elbow concurrent with HO from  
86 December 2010 to May 2024 at our hospital. The inclusion criteria were the following:  
87 (1) post-traumatic elbow stiffness resulting in functional debilitation, defined as a  
88 flexion contracture of  $\geq 30^\circ$  or further flexion limitation of  $\leq 130^\circ$ ; (2) elbow HO  
89 diagnosed based on radiographic workup; (3) complete clinical record and CT data; and

(4) aged 18 years or older. Elbows that fulfilled the above inclusion criteria with intra-articular injuries were included if radiographic assessments confirmed a congruent articular surface and an intact joint space, indicating that fracture healing did not adversely affect ulnohumeral motion. The exclusion criteria were the following: (1) immature bone; (2) insufficient clinical or radiographic data; (3) association with burns or central nervous system injuries; (4) other factors that might manifest as the primary features of elbow stiffness, such as scarred skin, incongruent joint surfaces, trauma-associated non-union, or malunion of the elbow; (5) other potential factors blocking elbow motion, such as loose bodies in the olecranon fossa; and (6) severe articular deformity with indistinct articular anatomy.

A total of 95 hospitalized patients who underwent surgical excision of HO for post-traumatic elbow stiffness were identified from the case system. Of these, 54 underwent open arthrolysis and 41 underwent arthroscopic arthrolysis. After applying our inclusion and exclusion criteria, 56 patients remained for analysis. Of the 95 patients, 39 were disqualified based on the following reasons: age younger than 18 years ( $n = 4$ ), unavailable preoperative CT performed at another hospital ( $n = 1$ ), controversial diagnosis of immature HO with small hazy display ( $n = 5$ ), low-quality CT images with dark and bright streaks from metal implants masking the majority of anatomical structures ( $n = 14$ ), association with traumatic brain injury ( $n = 2$ ), elbow joint malunion or nonunion ( $n = 5$ ), severe joint surface damage ( $n = 4$ ), severe deformity with indistinct articular anatomy ( $n = 1$ ), and presence of loose bodies or fragment debris immediately after trauma ( $n = 3$ ). Thus, the remaining 56 patients were deemed eligible



112 and included in the study. A flowchart of enrollment and exclusion is shown in **Figure**  
113 **1**.

114 The study group included 37 men (66.1%) and 19 women (33.9%) with elbow stiffness  
115 and defined HO after trauma. The mean age was 41 years (range, 19–74 years), and  
116 stiffness in the dominant arm was present in 31 patients (55.3%). The mean injury  
117 duration was 19 months (range, 3–144 months), and the most common original injury  
118 type was simple elbow dislocation (20 of 56, 35.7%), followed by injuries associated  
119 with distal humerus fractures (12 of 56, 21.4%) (**Table 1**).

#### 120 **CT-based radiographic analysis of HO**

121 The most recent CT scans before stiff elbow surgery were evaluated by two independent  
122 observers: an upper extremity fellowship-trained surgeon and a research fellow with  
123 clinical experience in HO treatment. Each observer studied the CT scans combined with  
124 three-dimensional CT (3D CT) of the participants independently and blindly following  
125 the same research protocol to identify, evaluate, and categorize the HO. One observer  
126 reviewed the images first, and then the second observer conducted two separate  
127 evaluations of the images with a time interval of one month to minimize potential bias.  
128 HO was defined as new bone formation that was not visible on radiographs taken  
129 immediately after the trauma, explicitly excluding any correspondence with fracture  
130 fragments.<sup>12</sup> The presence of HO in the elbow joint was documented using anatomical  
131 regions and bony landmarks as references in each respective region.<sup>12, 21, 22, 32, 33</sup> The  
132 observers evaluated the anatomical positions of the detected HO on the 3D CT images  
133 and CT scans set to a bone window (level: 800 Hounsfield units [HU]; width: 2000

134 HU). The following categories were used as a primary assessment of HO location: (1)  
 135 Posterior - olecranon tip; (2) Posteromedial - medial gutter; (3) Posterolateral - lateral  
 136 gutter; (4) Medial - medial epicondyle; (5) Lateral - lateral epicondyle; (6) Anterior -  
 137 humeroulnar joint; (7) Anterior - humeroradial joint (**Table 2**).

138 The sublime tubercle on the medial aspect of the coronoid process, where the ulnar  
 139 footprint of the ulnar collateral ligament (UCL) inserts, was used as a prominent bony  
 140 landmark to separate the medial and posteromedial aspects of the elbow joint.<sup>1</sup> Thus,  
 141 the medial gutter was defined as the bony region within the posteromedial compartment,  
 142 posteriorly from the anterior band of the UCL as the border. Similarly, the supinator  
 143 tubercle on the lateral surface of the ulna, where the lateral ulnar collateral ligament  
 144 (LUCL) attaches, was used as the bony landmark to separate the lateral and  
 145 posterolateral aspects of the elbow.<sup>5, 10</sup> The lateral gutter was defined as the bony region  
 146 within the posterolateral compartment lying posterior to the LUCL. A subsequent  
 147 analysis was conducted to analyze the positional relationship between the HO and the  
 148 periarticular muscle-tendon units. The same review procedure was applied to 2D CT  
 149 imaging, with the window settings adjusted to a soft-tissue window (level: 60 HU;  
 150 width: 360 HU) to enhance the visualization of periarticular muscles and tendons in  
 151 relation to the identified HO in the categorized anatomical regions.

152 The periarticular muscles, with tendinous insertions at specific bone landmarks within  
 153 the elbow joint, were used as references (**Table 2**). The following muscles were  
 154 included:

155 (1) The distal triceps brachii, which has its tendinous insertion on the olecranon.<sup>31</sup>

- 156 (2) The flexor carpi ulnaris (FCU), originating from the medial epicondyle and the  
 157 medial aspect of the olecranon.<sup>13</sup>
- 158 (3) The anconeus muscle, which arises from the dorsal side of the lateral epicondyle  
 159 of the humerus to the posterolateral aspect of the ulna.<sup>16</sup>
- 160 (4) The other flexor-pronator muscles, which form common tendons attached to the  
 161 medial epicondyle. This group includes the pronator teres (PT), flexor carpi  
 162 radialis (FCR), palmaris longus (PL), and flexor digitorum superficialis (FDS)  
 163 muscles.<sup>13</sup>
- 164 (5) The extensor muscles, which develop common extensor tendons attached to the  
 165 lateral epicondyle of the distal humerus.<sup>5</sup>
- 166 (6) The brachialis muscle, which originates from the anterior aspect of the distal  
 167 humerus and inserts into the tuberosity on the ulnar.<sup>30</sup>
- 168 (7) The supinator muscle, with its superficial head arising from the lateral  
 169 epicondyle and inserting on the lateral, posterior, and anterior surfaces of the  
 170 proximal radius.<sup>11</sup>

171

172 The margins of muscles or tendons, where HO is distributed and extended, were traced.

173 Three slices of the CT images were documented to illustrate the positional relationship

174 between the distribution of HO and the related muscle-tendon units. A muscle-guided

175 classification was then defined with the following categories:

176

- 177 **(1) Posterior - olecranon tip - triceps brachii (P-O-T)**

178 At the posterior aspect, the distal triceps brachii served as the reference muscle. The  
179 average distance from the most proximal edge of the tendon insertion to the tip of the  
180 olecranon is 14.8 mm.<sup>18, 19</sup> HO formed in the region between the triceps and olecranon  
181 was categorized and recorded as “Posterior - olecranon tip - triceps brachii (P-O-T)”  
182 **(Figure 2).**

183

### 184 **(2) Posteromedial - medial gutter - FCU (PM-MG-FCU)**

185 At the medial aspect of the distal humerus, the flexor-pronator muscles (FPMs) develop  
186 a common flexor insertion at the medial epicondyle of the humerus. However, their  
187 tendinous attachments on the proximal ulna are distinctly different. Specifically, the  
188 FCU exhibits a distinct tendinous insertion posterior to the sublime tubercle, with  
189 muscle fibers extending posteriorly along the oblique bundle of the UCL and  
190 distributing near the medial gutter of the posteromedial compartment.<sup>9, 13</sup> Thus, the  
191 FCU was used as the reference muscle in the posteromedial region. HO located within  
192 the posteromedial region near the medial gutter and FCU was categorized and recorded  
193 as “Posteromedial - medial gutter - FCU (PM-MG-FCU)” **(Figure 3).**

194

### 195 **(3) Posterolateral - lateral gutter – anconeus (PL-LG-AN)**

196 The anconeus muscle, originating at the posterosuperior aspect of the lateral epicondyle  
197 and inserting on the posterolateral surface of the proximal ulna, was used as the  
198 reference muscle in the posterolateral region **(Figure 4).**

199

**(4) Medial - medial epicondylar – flexor muscles (M-ME-FLEX)**

Compared to the FCU, other flexor muscles are positioned more anteriorly at the medial aspect of the elbow. The deep layers of the FPMs, including the FDS and pronator teres, develop attachments to the ulna just medial to the ulnar ridge, with fibers extending along the anterior bundle of the UCL.<sup>13</sup> Therefore, other muscles within the flexor-pronator mass, in addition to the FCU, served as reference muscles at the medial aspect of the elbow. HO formed between these flexors and medial epicondyle was categorized and documented as “Medial - medial epicondylar – flexor muscles (M-ME-FLEX)” (Figure 5).

**(5) Lateral - lateral epicondylar – extensor muscles (L-LE-EXT)**

To the lateral side of the elbow joint, the extensor muscles, featuring a typical tendinous structure attached to the lateral epicondyle, served as the reference muscles.<sup>5</sup> HO found between the extensor muscles and the lateral epicondyle was categorized and documented as “Lateral - lateral epicondylar – extensor muscles (L-LE-EXT)” (Figure 6).

**(6) Anterior - humeroulnar joint – brachialis (A-HU-B)**

To the anteromedial aspect of the elbow, the brachialis muscle, spanning along the humeroulnar joint, served as the reference muscle (Figure 7).

**(7) Anterior - humeroradial – supinator (A-HR-SP)**

222 To the anterolateral aspect of the elbow, the supinator was used as the reference muscle,  
223 which spans the humeroradial joint (**Figure 8**).

224

225 The severity of the HO was assessed using a radiographic classification system recently  
226 developed by Foruria et al that describes the relation between HO severity on CT  
227 images.<sup>12</sup> Severity was graded as follows in this study: 1 (hazy or scattered HO, with  
228 small to moderate size), 2 (extensive mature HO nearly bridging two separate bones),  
229 and 3 (complete bone bridge formation)<sup>12</sup> (**Figure 9**).

230

231 The time interval from the trauma to the recorded time of the most recent CT  
232 examination was considered the injury duration for cases of stiff elbow with HO.

233

#### 234 **Statistical analysis**

235 Descriptive statistics were performed using absolute and relative frequencies to depict  
236 the characteristics of HO distribution and radiographic severity within each category of  
237 the muscle-guided classification system.

238 Cohen's Kappa coefficient ( $\kappa$ ) was used to assess intra- and interobserver reliability  
239 regarding HO severity and localization.<sup>24</sup> According to Landis and Koch's criteria,  
240 values were categorized as follows:  $\leq 0$  (no agreement), 0.01–0.20 (none to slight),  
241 0.21–0.40 (fair), 0.41–0.60 (moderate), 0.61–0.80 (substantial), and 0.81–1.00 (almost  
242 perfect agreement).<sup>23</sup>

243 To examine the correlation between radiographic severity, classified into three degrees,

244 and the seven categories of the muscle-guided classification for elbow HO, a 3×7  
 245 contingency table was used to present the association frequencies. Fisher's exact test  
 246 was performed to evaluate the frequencies and calculate the corresponding significance.  
 247 Spearman regression analysis was performed to investigate the relationship between  
 248 injury duration and the radiographic severity of HO located within the categorized  
 249 muscle-guided regions. A significance level of  $p < .05$  was defined.  
 250 Statistical analysis of the collected data was performed using the statistical software  
 251 SPSS Statistics (version 25; IBM, Armonk, NY, USA). A significance level of  $p < .05$   
 252 was defined for the above statistical analysis.

## 253 254 255 **Results**

256 The most common HO localization was at PM-MG-FCU in 38 patients (67.9%)  
 257 according to the muscle-guided classification. The next most common localization was  
 258 at P-O-T in 32 patients (57.1%), M-ME-FLEX in 27 (48.2%), A-HU-B in 24 (42.9%),  
 259 L-LE-EXT in 21 (37.5%), PL-LG-AN in 17 (30.4%), and A-HR-SP in 8 (14.3%)  
 260 (**Figure 10**).

261 **Table 3** summarizes the occurrence of HO at various locations across different original  
 262 injury types. According to Fisher's exact test, no significant difference was observed in  
 263 the distribution of locations categorized based on the muscle-guided classification  
 264 across different injury types ( $\chi^2 = 41.581$ ,  $p = .811$ ).

265 A 3×7 contingency table was created to display the constituent ratio of three  
 266 radiographic severity grades in seven categories of the muscle-guided classification.

267 According to the results of Fisher's exact test, there was a significant correlation  
 268 between the radiographic severity and the location categorized by the muscle-guided  
 269 classification ( $\chi^2 = 32.039$ ,  $p < .001$ ). Pairwise comparisons following the Kruskal-  
 270 Wallis test further showed that the formation rate of extensive mature HO, characterized  
 271 by almost complete or complete bridging of two separate bones in the radiographic  
 272 images (grades 2 and 3 of radiographic severity), was significantly higher in regions  
 273 categorized as PI-LG-AN (41.2%), P-O-T (40.6%), and PM-MG-FCU (39.5%)  
 274 compared to M-ME-FLEX (0%). The p-values, adjusted by the Bonferroni correction,  
 275 were .047, .007, and .007, respectively. Furthermore, the formation rate of extensive  
 276 mature HO in the regions categorized as P-O-T (40.6%) and PM-MG-FCU (39.5%)  
 277 was significantly higher than in the L-LE-EXT (0%) (adjusted p-values of .019 and .018,  
 278 respectively). However, the HO formation rates in the anterior compartment of the  
 279 elbow joint involving A-HU-B (16.7%) and A-HR-SP (37.5%) were moderate and did  
 280 not show a significant difference compared to the other five categories. There was no  
 281 significant relationship between injury duration and radiographic severity ( $p = .109$ )  
 282 The interobserver reliability for the HO location was substantial, with a kappa ( $\kappa$ ) value  
 283 of 0.739 ( $p < .001$ ). For HO severity, it was also substantial, with a  $\kappa$  value of 0.651 ( $p$   
 284  $< .001$ ). Additionally, the intraobserver reliability for the HO location was almost perfect,  
 285 with a  $\kappa$  value of 0.890 ( $p < .001$ ). For HO severity, it is almost perfect as well, with a  $\kappa$   
 286 value of 0.848 ( $p < .001$ ).

287

## 288 Discussion

289 Previous radiographic studies on post-traumatic elbow HO were based on anatomical



regions or specific bony landmarks in plain radiographs.<sup>22</sup> Foruria et al classified the locations of HO in the post-traumatic elbow based on the relative position to bony components such as the humerus, radius, and ulna.<sup>12</sup> Zhang et al categorized the HO locations in the elbow as lateral/medial supracondylar areas, lateral/medial aspects of the capsule, and proximal radius/ulna.<sup>33</sup> While these studies described the information based on general location, the authors did not specify the localization relative to the periarticular soft tissue, which is the main pathology of post-traumatic HO.<sup>8</sup>

Although HO is currently defined as new bone formed within extra-skeletal soft tissues, no further investigation of the positional relationship between soft tissue and HO has been described.<sup>8, 17</sup> A recent study demonstrated that injured Achilles tendons in animal models can develop HO that exhibits specific spatiotemporal patterns during healing.<sup>29</sup> Microtomography revealed that a small HO initially forms at the stump of the torn tendon near the bone site and subsequently extends along the muscle following the direction of the tendon's main axes. The study also identified similarities in HO deposits between rats and humans through a review of clinical CT images from 38 patients with Achilles tendon injuries. In a clinical study on HO in post-traumatic elbows, Foruria et al proposed that HO location is likely correlated with the injury pattern, often developing at the origins of torn soft-tissue structures or near fracture sites. Their results are consistent with HO being more prevalent in areas with extensive soft-tissue injury. Therefore, to contribute new insights into the mechanisms of HO formation and effectively treat and prevent HO after elbow trauma, further investigation is necessary to achieve a more precise mapping of HO localization and determine its position near

312 soft tissue in post-traumatic elbows with greater precision.

313 In the present study, we introduced a novel muscle-guided classification system to  
314 precisely determine the positional relationship between HO and the periarticular  
315 muscle-tendon units in the elbow joint. This classification system provided a detailed  
316 depiction of HO detected in the CT images using anatomical references such as muscle-  
317 tendon units and bony landmarks. The system identified seven categories based on  
318 prominent reference muscles distributed near the elbow joint: triceps, FCU, FDS along  
319 with other flexor muscles, extensor muscles, anconeus, brachialis, and supinator. This  
320 approach allowed a more accurate localization and mapping of HO relative to the soft  
321 tissue in the elbow joint. CT was effective for determining the precise location of HO  
322 in a stiff elbow, including small, hazy HO categorized as grade 1 in radiographic  
323 severity classifications. CT also provided a detailed view of the complex architecture  
324 of articular surfaces, offering advantages over plain radiographs. We found that CT  
325 scans efficiently displayed HO location in soft tissue when using reference muscles  
326 with satisfactory observer reliability. Although MRI is useful for evaluating soft tissues  
327 near the elbow, it is less effective than CT in visualizing the bony details of structures  
328 such as HO and joint architecture. Additionally, using reference muscles to describe HO  
329 location provides three-dimensional spatial information about HO distribution based on  
330 muscle distribution and insertion in the elbow.

331 Among patients with symptomatic post-traumatic elbow stiffness from HO, 38 out of  
332 56 (67.9%) elbows developed HO in the posteromedial aspect of the elbow, specifically  
333 in the area between the FCU and the medial gutter, categorized as PM-MG-FCU. This

category exhibited the highest frequency among all categories in the muscle-guided classification, which is consistent with previous reports. Park et al reported that HO most commonly developed in the posterior aspect such as the posteromedial aspect of the capsule, occurring in 36 out of 40 (90%) individuals with elbow stiffness following trauma.<sup>27</sup> Foruria et al reported that HO was primarily distributed in the posterior aspect of the ulna following surgery for proximal radius and ulna fractures, with or without associated distal humeral fractures, occurring in 15 out of 48 elbows (31.3%).<sup>12</sup> Zhang et al reported a high HO prevalence in the posterior region of the ulna, in 31 out of 56 patients (55%), whereas the highest frequency of postoperative HO was observed in the medial aspect in 52 out of 56 patients. This may be because the authors divided the elbow region primarily based on bony landmarks in the coronal two-dimensional plane without clearly defining the posteromedial and medial regions. In the present study, the sublime tubercle, where the anterior band of the UCL inserts and separates the FDS and FCU, was used as a prominent landmark to demarcate the region between the posteromedial and medial areas.

The present study also assessed the radiographic severity of HO by referencing the classification system for elbow HO proposed by Foruria et al in 2013.<sup>12</sup> In contrast to the existing functional classification by Hastings and Graham,<sup>32</sup> assessment of HO severity in the present study predominantly focused on radiographic morphological characteristics.

Our results revealed a significant correlation between radiographic severity and HO location. The overall posterior compartment of the elbow presented a significantly

356 higher risk of developing extensive mature HO and bridging two separate bones (grade  
357 2 and 3 in radiographic severity) (Figure 3), specifically in the PL-LG-AN (41.2%), P-  
358 O-T (40.6%), and PM-MG-FCU (39.5%) categories. However, no grade 2 or 3  
359 radiographic severity of HO was observed in the medial or lateral aspects of the elbow  
360 involving the M-ME-FLEX and L-LE-EXT categories. These results suggest a varying  
361 susceptibility to develop severe, massive HO in different areas of the elbow.

362 Based on the positional relationships observed between HO and surrounding muscle-  
363 tendon units on CT images, HO was mostly located at tendinous insertion points and  
364 extended directionally along the respective muscles. Interestingly, images obtained  
365 from several patients revealed small, limited HO formations in tendons near their bony  
366 insertions (Figure 6). These observations suggested that HO development in the elbow  
367 may exhibit a specific spatial pattern, similar to findings by Pierantoni et al regarding  
368 the Achilles tendon.<sup>29</sup>

369 The present study demonstrated substantial to almost perfect inter- and intraobserver  
370 reliability for both HO location and severity. This reliability underscores the validity of  
371 the muscle-guided classification system in clinical practice and research settings.

372 Understanding the precise location where HO forms and extends in the elbow joint  
373 could significantly advance research on the mechanisms of HO formation and improve  
374 treatment strategies. For instance, this knowledge could aid in localizing HO during  
375 surgery<sup>4</sup> and identifying specific muscles affected by HO for targeted botulinum toxin  
376 injections as part of HO treatment and prevention strategies.<sup>2</sup> Furthermore, the use of a  
377 standardized nomenclature can improve the determination of HO location on CT scans

378 and refine preoperative surgical planning.

379 This study has several limitations. First, there was a selection bias as it included only  
380 patients with elbow stiffness who underwent surgical treatment. Additionally, because  
381 of the nature of the study, few cases had both available MRI images and CT scans from  
382 the same time point. Future studies will benefit from image registration or fusion  
383 techniques for CT and MR images to better illustrate the correlation between HO  
384 location and soft tissue involvement.

385

## 386 **Conclusion**

387 A novel muscle-guided classification system was developed to effectively characterize  
388 HO distribution near muscle-tendon units in post-traumatic elbows. The HO in the PM-  
389 MG-FCU category was the most prevalent, occurring in 38 patients (67.9%), the highest  
390 frequency among all classifications. HO located in the posterior compartment,  
391 particularly involving specific muscle-tendon units such as the anconeus, triceps brachii,  
392 and FCU, was associated with a higher risk of greater radiographic severity. These  
393 findings improve our understanding of HO distribution near soft tissue in post-  
394 traumatic elbow stiffness and may potentially inform more targeted therapeutic  
395 strategies.

396

## 397 **References**

- 398 1. Al-Ani Z, Wright A, Ricks M, Watts AC. Posteromedial rotatory instability of  
399 the elbow: What the radiologist needs to know. *Eur J Radiol* 2021;141:109819.  
400 doi:10.1016/j.ejrad.2021.109819  
401 2. Ausk BJ, Gross TS, Bain SD. Botulinum Toxin-induced Muscle Paralysis

- 402        Inhibits Heterotopic Bone Formation. Clin Orthop Relat Res 2015;473(9):2825-  
403        30. doi:10.1007/s11999-015-4271-4
- 404    3.    Avci O, Röhrle O. Determining a musculoskeletal system's pre-stretched state  
405        using continuum-mechanical forward modelling and joint range optimization.  
406        Biomech Model Mechanobiol 2024;23(3):1031-53. doi:10.1007/s10237-024-  
407        01821-x
- 408    4.    Ben H, Kholinne E, Zeng CH, Alsaqri H, Lee JB, So SP, et al. Prevalence,  
409        Timing, Locational Distribution, and Risk Factors for Heterotopic Ossification  
410        After Elbow Arthroscopy. Am J Sports Med 2023;51(13):3401-8.  
411        doi:10.1177/03635465231198862
- 412    5.    Bernholt DL, Rosenberg SI, Brady AW, Storaci HW, Viola RW, Hackett TR.  
413        Quantitative and Qualitative Analyses of the Lateral Ligamentous Complex and  
414        Extensor Tendon Origins of the Elbow: An Anatomic Study. Orthop J Sports  
415        Med 2020;8(10):2325967120961373. doi:10.1177/2325967120961373
- 416    6.    Casavant AM, Hastings H, 2nd. Heterotopic ossification about the elbow: a  
417        therapist's guide to evaluation and management. J Hand Ther 2006;19(2):255-  
418        66. doi:10.1197/j.jht.2006.02.009
- 419    7.    Chen S, Yu SY, Yan H, Cai JY, Ouyang Y, Ruan HJ, Fan CY. The time point in  
420        surgical excision of heterotopic ossification of post-traumatic stiff elbow:  
421        recommendation for early excision followed by early exercise. J Shoulder  
422        Elbow Surg 2015;24(8):1165-71. doi:10.1016/j.jse.2015.05.044
- 423    8.    Cherief M, Negri S, Qin Q, Pagani CA, Lee S, Yang YP, et al. TrkA+ Neurons  
424        Induce Pathologic Regeneration After Soft Tissue Trauma. Stem Cells Transl  
425        Med 2022;11(11):1165-76. doi:10.1093/stcltm/szac073
- 426    9.    Cinque ME, Schickendantz M, Frangiamore S. Review of Anatomy of the  
427        Medial Ulnar Collateral Ligament Complex of the Elbow. Curr Rev  
428        Musculoskelet Med 2020;13(1):96-102. doi:10.1007/s12178-020-09609-z
- 429    10.    Desouky AM, Atiyya AN, Elbishbishi M, Sawy MME. A modified trans-  
430        anconeus approach to facilitate fixation of a posterior radial head fracture: a  
431        cadaveric feasibility study. Anat Cell Biol 2023;56(1):39-45.



- doi:10.5115/acb.22.201
11. Erak S, Day R, Wang A. The role of supinator in the pathogenesis of chronic lateral elbow pain: a biomechanical study. *J Hand Surg Br* 2004;29(5):461-4. doi:10.1016/j.jhsb.2004.06.001
  12. Foruria AM, Augustin S, Morrey BF, Sánchez-Sotelo J. Heterotopic ossification after surgery for fractures and fracture-dislocations involving the proximal aspect of the radius or ulna. *J Bone Joint Surg Am* 2013;95(10):e66. doi:10.2106/jbjs.K.01533
  13. Frangiamore SJ, Moatshe G, Kruckeberg BM, Civitaresse DM, Muckenhirn KJ, Chahla J, et al. Qualitative and Quantitative Analyses of the Dynamic and Static Stabilizers of the Medial Elbow: An Anatomic Study. *Am J Sports Med* 2018;46(3):687-94. doi:10.1177/0363546517743749
  14. Green DP, McCoy H. Turnbuckle orthotic correction of elbow-flexion contractures after acute injuries. *J Bone Joint Surg Am* 1979;61(7):1092-5.
  15. Ilahi OA, Bennett JB, Gabel GT, Mehlhoff TL, Kohl HW, 3rd. Classification of heterotopic ossification about the elbow. *Orthopedics* 2001;24(11):1075-7; discussion 7-8. doi:10.3928/0147-7447-20011101-20
  16. Jiménez-Díaz V, Aragonés P, García-Lamas L, Barco-Laakso R, Quinones S, Korschake M, et al. The anconeus muscle revisited: double innervation pattern and its clinical implications. *Surg Radiol Anat* 2021;43(10):1595-601. doi:10.1007/s00276-021-02750-5
  17. Kang H, Strong AL, Sun Y, Guo L, Juan C, Bancroft AC, et al. The HIF-1 $\alpha$ /PLOD2 axis integrates extracellular matrix organization and cell metabolism leading to aberrant musculoskeletal repair. *Bone Res* 2024;12(1):17. doi:10.1038/s41413-024-00320-0
  18. Keener JD, Chafik D, Kim HM, Galatz LM, Yamaguchi K. Insertional anatomy of the triceps brachii tendon. *J Shoulder Elbow Surg* 2010;19(3):399-405. doi:10.1016/j.jse.2009.10.008
  19. Kholinne E, Kwak JM, Heo Y, Hwang SJ. The anatomic - magnetic resonance imaging study of distal triceps brachii tendon. *J Orthop Surg (Hong Kong)*

- 2022;30(3):10225536221122262. doi:10.1177/10225536221122262
20. Kwak JM, Rotman D, Lievano JR, Xue M, O'Driscoll SW. The role of the lateral part of the distal triceps and the anconeus in varus stability of the elbow: a biomechanical study. *J Shoulder Elbow Surg* 2023;32(1):159-67. doi:10.1016/j.jse.2022.08.005
21. Lee KB, Cho YJ, Park JK, Song EK, Yoon TR, Seon JK. Heterotopic ossification after primary total ankle arthroplasty. *J Bone Joint Surg Am* 2011;93(8):751-8. doi:10.2106/jbjs.J.00178
22. Leyder D, Döbele S, Konrads C, Histing T, Fischer CS, Ahrend MD, Ziegler P. Classification and Incidence of Heterotopic Ossifications in Relation to NSAID Prophylaxis after Elbow Trauma. *J Clin Med* 2024;13(3). doi:10.3390/jcm13030667
23. McHugh ML. Interrater reliability: the kappa statistic. *Biochem Med (Zagreb)* 2012;22(3):276-82. No doi
24. Meesters AML, Ten Duis K, Banierink H, Stirler VMA, Wouters PCR, Kraeima J, et al. What Are the Interobserver and Intraobserver Variability of Gap and Stepoff Measurements in Acetabular Fractures? *Clin Orthop Relat Res* 2020;478(12):2801-8. doi:10.1097/corr.0000000000001398
25. Moore JS. Function, structure, and responses of components of the muscle-tendon unit. *Occup Med* 1992;7(4):713-40.
26. Nimura A, Shimura H, Hoshika S, Fukai A, Akita K. Elbow anatomy in perspective of joint capsule and surrounding aponeuroses: a narrative review. *JSES Int* 2024;8(3):654-60. doi:10.1016/j.jseint.2024.01.006
27. Park MJ, Chang MJ, Lee YB, Kang HJ. Surgical Release for Posttraumatic Loss of Elbow Flexion. *JBJS Essent Surg Tech* 2011;1(3):e16. doi:10.2106/jbjs.St.K.00008
28. Pereira BP. Revisiting the anatomy and biomechanics of the anconeus muscle and its role in elbow stability. *Ann Anat* 2013;195(4):365-70. doi:10.1016/j.aanat.2012.05.007
29. Pierantoni M, Hammerman M, Silva Barreto I, Larsson D, Notermans T, Bodey



- 492 AJ, et al. Spatiotemporal and microstructural characterization of heterotopic  
 493 ossification in healing rat Achilles tendons. *Faseb j* 2023;37(6).  
 494 doi:10.1096/fj.202201018RRR
- 495 30. Plantz MA, Bordoni B. Anatomy, Shoulder and Upper Limb, Brachialis Muscle.  
 496 StatPearls. Treasure Island (FL): StatPearls Publishing. © 2024, StatPearls  
 497 Publishing LLC.; 2024.
- 498 31. Tiwana MS, Sinkler MA, Bordoni B. Anatomy, Shoulder and Upper Limb,  
 499 Triceps Muscle. StatPearls. Treasure Island (FL): StatPearls Publishing. © 2024,  
 500 StatPearls Publishing LLC.; 2024.
- 501 32. Viola RW, Hastings H, 2nd. Treatment of ectopic ossification about the elbow.  
 502 *Clin Orthop Relat Res* 2000(370):65-86.
- 503 33. Zhang W, Wu X, Chen H, Bai J, Long L, Xue D. Regional distribution  
 504 prevalence of heterotopic ossification in the elbow joint: a 3D study of patients  
 505 after surgery for traumatic elbow injury. *J Shoulder Elbow Surg*  
 506 2024;33(4):948-58. doi:10.1016/j.jse.2023.11.015

507

508 **Figure Legends**

509 **Figure 1.** Flowchart of enrollment and exclusion. HO, heterotopic ossification; CT,  
 510 computed tomography.

511 **Figure 2.** The Posterior - olecranon tip - triceps brachii (P-O-T) category in the muscle-  
 512 guided classification system. The Posterior - olecranon tip - triceps brachii (P-O-T)  
 513 category in the muscle-guided classification system. The HO in the posterior region is  
 514 marked in green in the 3D CT image. The extended large HO in the sagittal 2D scan is  
 515 marked with red asterisks and the small HO is indicated by a red arrowhead. The  
 516 tendinous insertion of the triceps brachii muscle is indicated by a yellow single arrow,  
 517 and the belly of the triceps brachii muscle is indicated by blue triple arrows.

518 **Figure 3.** The Posteromedial - medial gutter - flexor carpi ulnaris (PM-MG-FCU)  
 519 category in the muscle-guided classification system. The HO in the posteromedial  
 520 region is marked in green in the 3D CT image. The extended large HO in the axial 2D  
 521 scan is marked with red asterisks and the small HO is indicated by a red arrowhead.

522 The tendinous insertion of the flexor carpi ulnaris (FCU) on the ulna is indicated by a  
 523 yellow single arrow, and the belly of the FCU muscle is indicated by blue triple arrows.

524 **Figure 4.** The Posterolateral - lateral gutter – anconeus (PL-LG-AN) category in the  
 525 muscle-guided classification system. The HO in the posterolateral region is marked in  
 526 green in the 3D CT image. The extended large HO in the axial 2D scan is marked with  
 527 red asterisks. The tendinous insertion of the anconeus on the ulna is indicated by a  
 528 yellow single arrow, and the belly of the anconeus muscle is indicated by blue triple  
 529 arrows.

530 **Figure 5.** The Medial - medial epicondylar – flexor muscles (M-ME-FLEX) category  
 531 in the muscle-guided classification system. The HO located at the medial aspect is  
 532 marked in green in the 3D CT image. The small, limited HO in the coronal 2D scan is  
 533 marked with red arrowheads. The common tendinous insertion of the flexor muscles on  
 534 the medial epicondylar of the humerus is indicated by a yellow single arrow.

535 **Figure 6.** The Lateral - lateral epicondylar – extensor muscles (L-LE-EXT) category in  
 536 the muscle-guided classification system. The HO located at the lateral aspect is marked  
 537 in green in the 3D CT image. The small, limited HO in the coronal 2D scan is marked  
 538 with red arrowheads. The common tendinous insertion of the extensor muscles on the  
 539 lateral epicondylar of the humerus is indicated by a yellow single arrow, and the belly  
 540 of the extensor muscles is indicated by blue triple arrows.

541 **Figure 7.** The Anterior - humeroulnar joint – brachialis (A-HU-B) category in the  
 542 muscle-guided classification system. The HO in the anteromedial aspect is marked in  
 543 green in the 3D CT image. The HO in the sagittal 2D scan is marked with red asterisks.  
 544 The insertion of the brachialis muscle on the anterior ulna is indicated by a yellow single  
 545 arrow, and the belly of the brachialis muscle is indicated by blue triple arrows.

546 **Figure 8.** The Anterior - humeroradial – supinator (A-HR-SP) category in the muscle-  
 547 guided classification system. The HO in the anterolateral aspect is marked in green in  
 548 the 3D CT image. The HO in the 2D scan is marked with red asterisks. The distribution  
 549 of the supinator muscle is indicated by blue triple arrows.

550 **Figure 9.** The sagittal 2D CT scan of HO in the Posterior - olecranon tip - triceps brachii  
 551 (P-O-T) category illustrates the three levels of HO severity: Grade 1, hazy or scattered

552 HO, with small to moderate size; Grade 2, extensive mature HO nearly bridging two  
 553 separate bones; Grade 3, complete bone bridge formation.

554 **Figure 10.** A frequency distribution shows the exact number of HO cases grouped by  
 555 muscle-guided classification, as well as the count of each of the three levels of  
 556 radiographic severity within the different HO categories. PM-MG-FCU, Posteromedial  
 557 - medial gutter - flexor carpi ulnaris; P-O-T, Posterior - olecranon tip - triceps brachii;  
 558 M-ME-FLEX, Medial - medial epicondylar – flexor muscles; A-HU-B Anterior -  
 559 humeroulnar joint – brachialis; L-LE-EXT, Lateral - lateral epicondylar – extensor  
 560 muscles; PL-LG-AN, Posterolateral - lateral gutter – anconeus; A-HR-SP, Anterior -  
 561 humeroradial – supinator.

562

#### 563 **Table Legends**

564 **Table 1.** Demographics and injury characteristics of patients

565 **Table 2.** Anatomic regions and bony landmarks for primary assessment of HO  
 566 location

567 **Table 3.** Distribution of locations of heterotopic ossification among original injury  
 568 patterns

569

**TABLE 1**  
Demographics and injury characteristics of the patients

Characteristics	Values or proportions
Number of patients, n	56
Male, n	37 (66.1)
Age, mean (range), years	41, 19-74
Dominant arm, n	31 (55.3)
Injury duration* mean (range), months	19, 3-44
Original injury treatment, n	
Surgical treatment	39 (69.6)
Nonoperative management	17 (30.4)
Original injury types, n	
Simple elbow dislocation	20 (35.7)
Injuries with associated distal humeral fracture	12 (21.4)
Isolated radial head/neck fracture	8 (14.3)
Terrible triad injury	6 (10.7)
Isolated olecranon fracture	3 (5.4)
coronoid fracture associated with elbow dislocation	3 (5.4)
Transolecranon fracture-dislocation	2 (3.6)
Monteggia fracture-dislocation	1 (1.8)
olecranon with concomitant radial head fracture	1 (1.8)
Surgical approach for elbow arthrolysis, n	
Open arthrolysis	30 (53.6)
Arthroscopic arthrolysis	26 (46.4)

\* The time interval between the occurrence of the traumatic injury and the most recent recorded CT examination

**TABLE 2**Anatomic Regions and Bony Landmarks for Primary Assessment of HO Location<sup>1</sup>

	<b>Anatomical regions</b>	<b>Bony Landmarks</b>	<b>Muscle-Tendon Units</b>
<b>1</b>	Posterior	Olecranon tip	Triceps
<b>2</b>	Posteromedial	Medial gutter	FCU
<b>3</b>	Posterolateral	Lateral gutter	Anconeus
<b>4</b>	Medial	Medial humeral epicondyle	Flexor Muscles (FCR, FDS, pronator)
<b>5</b>	Lateral	Lateral humeral epicondyle	Extensor muscles
<b>6</b>	Anteromedial	Humeroulnar joint line	Brachialis
<b>7</b>	Anterolateral	Humeroradial joint line	Supinator

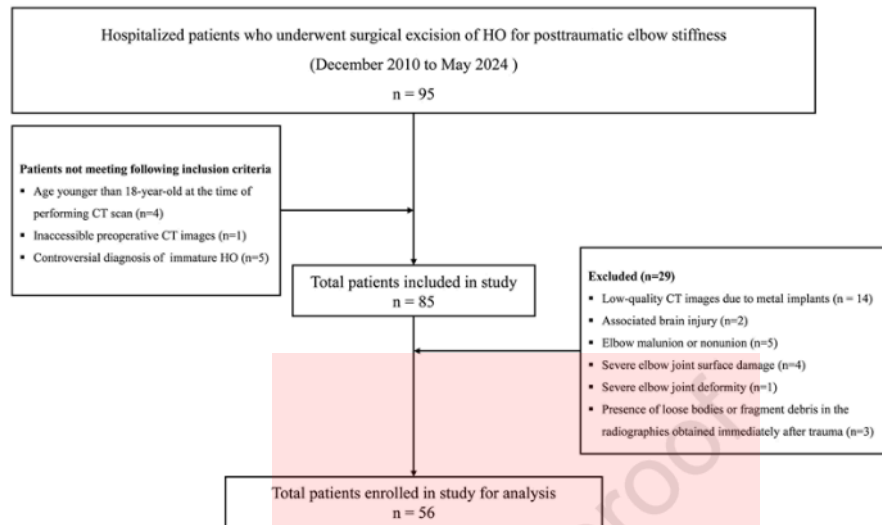
<sup>1</sup>FCU, flexor carpi ulnaris; FDS, flexor digitorum superficialis

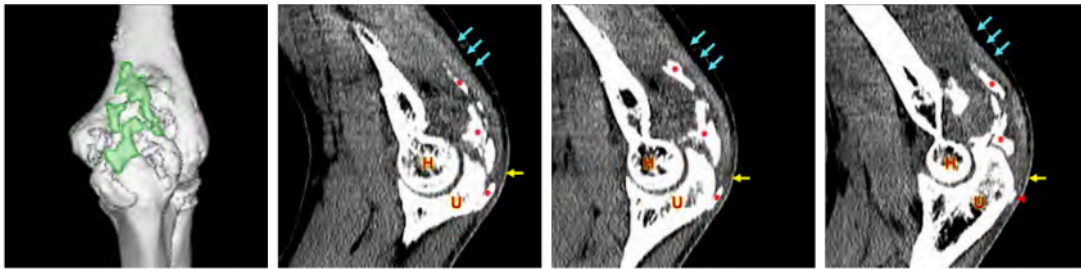
**TABLE 3**

Distribution of Locations of Heterotopic Ossification Among Original Injury Patterns

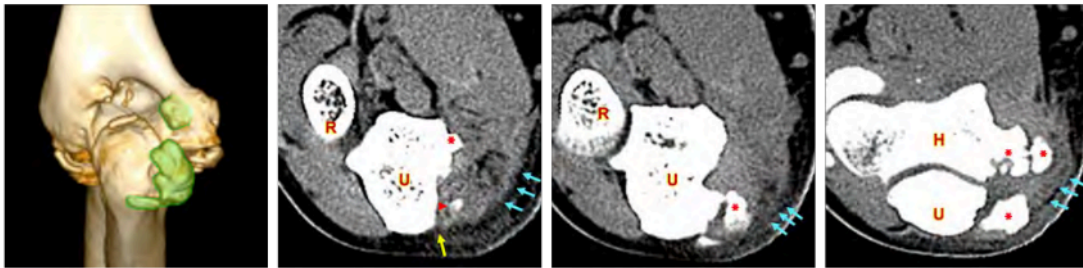
Original Injury Types	HO Cases	Categories of HO Location*						
		P-O-T	PM-MG-FCU	PL-LG-AN	M-ME-FLEX	L-LE-EXT	A-HU-B	A-HR-SP
Simple elbow dislocation	20 (35.7%)	14	14	5	13	9	8	4
Injuries with associated distal humeral fracture	12 (21.4%)	8	7	4	4	0	6	1
Isolated radial head/neck fracture	8 (14.3%)	4	5	2	5	6	3	0
Terrible triad injury	6 (10.7%)	4	4	4	2	5	5	3
Isolated olecranon fracture	3 (5.4%)	1	3	1	0	0	0	0
Coronoid fracture associated with elbow dislocation	3 (5.4%)	1	2	1	2	1	2	0
Transolecranon fracture-dislocation	2 (3.6%)	0	1	0	1	0	0	0
Monteggia fracture-dislocation	1 (1.8%)	0	1	0	0	0	0	0
Olecranon with concomitant radial head fracture	1 (1.8%)	0	1	0	0	0	0	0

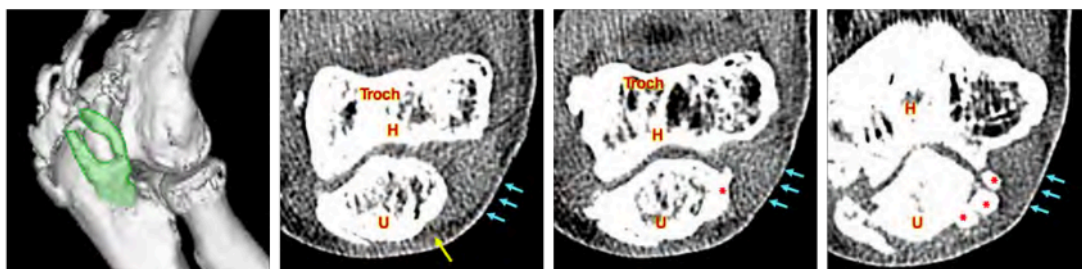
\* Categories of HO location are based on the muscle-guided classification as follows: Posterior - Olecranon tip - Triceps brachii (P-O-T); Posteromedial - Medial gutter - Flexor carpi ulnaris (PM-MG-FCU); Posterolateral - Lateral gutter - Anconeus (PL-LG-AN); Medial - Medial epicondylar - Flexor muscles (M-ME-FLEX); Lateral - Lateral epicondylar - Extensor muscles (L-LE-EXT); Anterior - Humeroulnar joint - Brachialis (A-HU-B); Anterior - Humeroradial - Supinator (A-HR-SP).



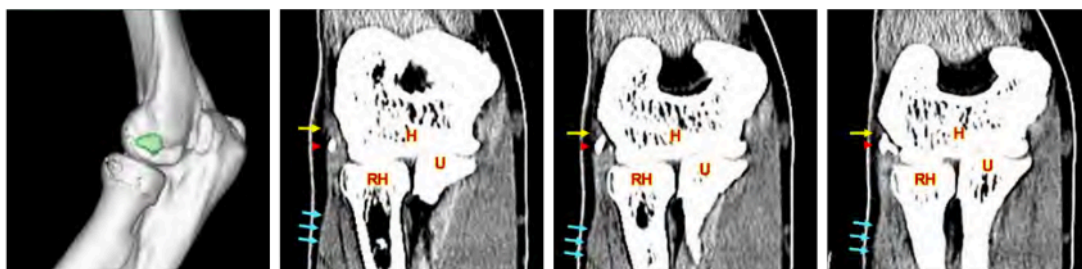


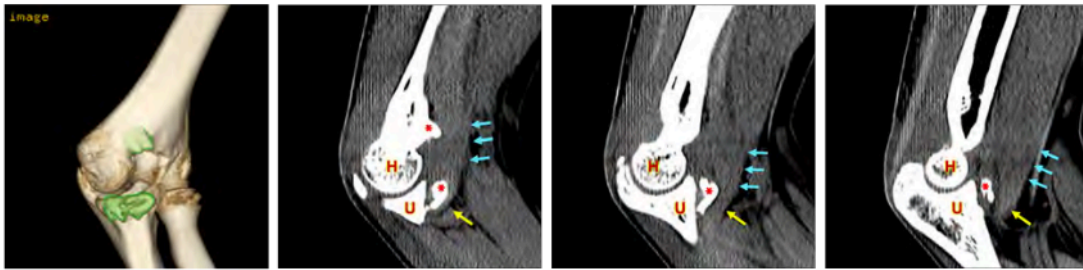


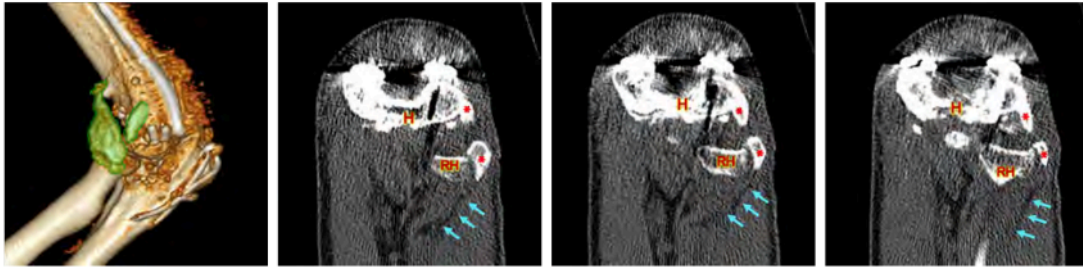


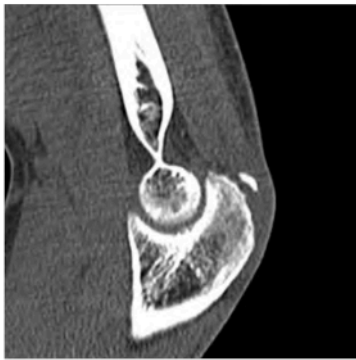




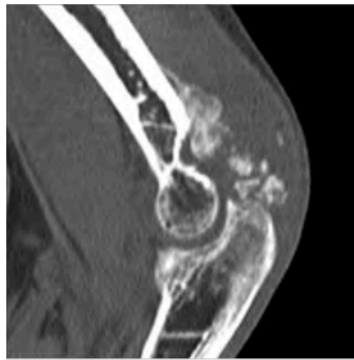








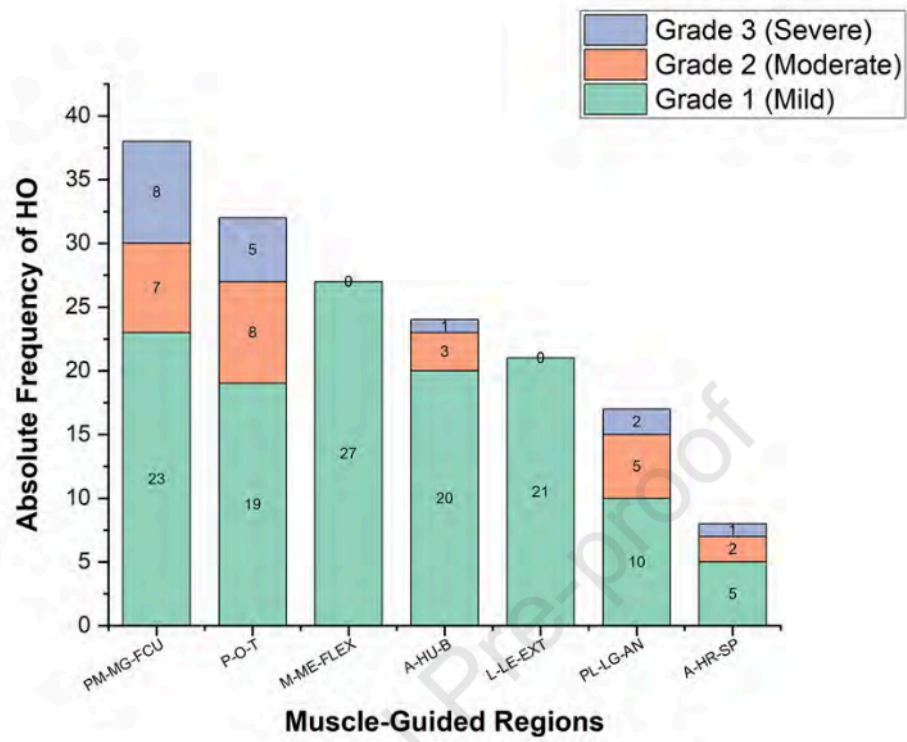
Grade 1



Grade 2



Grade 3





# 11. Hasil uji similaritas Muscle-Guided Mapping

ORIGINALITY REPORT

12%  
SIMILARITY INDEX

6%  
INTERNET SOURCES

11%  
PUBLICATIONS

6%  
STUDENT PAPERS

MATCH ALL SOURCES (ONLY SELECTED SOURCE PRINTED)

3%

★ Submitted to University of Hertfordshire  
Student Paper

Exclude quotes      On  
Exclude bibliography      On

Exclude matches      < 10 words